Available online at www.sciencedirect.com

ScienceDirect

Procedia CIRP 111 (2022) 92–96

www.elsevier.com/locate/procedia

12th CIRP Conference on Photonic Technologies [LANE 2022], 4-8 September 2022, Fürth, Germany

Laser Welding of L-PBF AM components out of inconel 718

Christian Brunner-Schwer[a], Juan Simón-Muzás[b,*], Max Biegler[a], Kai Hilgenberg[b], Michael Rethmeier[c,b,a]

[a]*Fraunhofer Institute for Production Systems and Design Techology IPK, Pascalstraße 8-9, 10587, Berlin, Germany*
[b]*Bundesanstalt für Materialforschung und –prüfung, Unter den Eichen, 87 12205, Berlin, Germany*
[c]*Institute of Machine Tools and Factory Management, Technische Universität Berlin, Pascalstraße 8-9, 10587, Berlin, Germany*

* Corresponding author. Tel.: +49 30 8104-4558; fax: +49 30 8104-1027. *E-mail address:* Juan.Simon-Muzas@bam.de

Abstract

With regard to efficient production, it is desirable to combine the respective advantages of additively and conventionally manufactured components. Particularly in the case of large-volume components that also include filigree or complex structures, it makes sense to divide the overall part into individual elements, which afterwards have to be joined by welding.
The following research represents a first step in fundamentally investigating and characterizing the joint welding of Laser Powder Bed Fusion (L-PBF) components made of Inconel 718. For this purpose, bead-on-plate welds were performed on plates manufactured using the L-PBF process and compared with the conventionally manufactured material. Conventional laser beam welding was used as welding process. The weld geometry was investigated as a function of the L-PBF build-up orientation. It was found that the welding depth and weld geometry differ depending on this orientation and in comparison to the conventional material.

Keywords: Laser Welding; L-PBF; Inconel 718; Weld geometry; Bead-on-plate welds

1. Introduction

Additive manufacturing processes can be used to produce components from a wide range of materials to near-net-shape dimensions. The advantages of the Laser Powder Bed Fusion (L-PBF) process, as one of the dominant technologies of metal additive manufacturing (AM), are described in many publications, e.g. [1]. Two factors that slow down the further spread of the technology are, on the one hand, limited component sizes due to limited build volumes and, on the other hand, comparatively low volume build rates, which in turn lead to long process times [2]. One consequence is that the manufacture and use of additive components is now particularly economical in series production if they are highly specialized, i.e., have complex features, e.g., ventilated turbine blades or bionic structures. Integration into conventional designs can then lead to significant increases in productivity, production time and material savings [3]. Such a combination of conventional and additively manufactured components combines the advantages of both approaches and is also referred to as a hybrid component [4].

The precipitation-hardenable nickel-based alloy Inconel 718 is characterized by high strength up to temperatures of 650°C and having a very good corrosion resistance. As a result, this alloy is often used in components that are exposed to high thermomechanical loads, such as in gas turbines or in aircraft engines [5]. Compared to other nickel-based alloys, this alloy is generally considered to have good weldability [6] and can therefore also be processed by the L-PBF process. Due to different contributing factors, such as heat input of the welding process [7] or heat treatment condition of the base material [8], cracks are prone to occur especially in the heat-affected zone (HAZ). Shinozaki et al. [9] draws a direct connection between

10.1016/j.procir.2022.08.072

the weld geometry and the occurrence of cracks in the HAZ. According to the study, the cracks occur mostly in the necked zone of the nail head like bead cross section and suggests that there is a critical radius of curvature in this area that determines whether cracks occur or not [9]. The formation of the weld geometry is directly dependent on the welding process parameters, in particular the heat input and the welding speed, whether with CO_2 lasers [9], Nd:YAG lasers [7, 10] or electron beam welding (EBW) [11] of wrought Inconel 718. Mei et al. [11] adds that the condition of the base material also has a significant influence on the weld geometry. They studied four different heat treatment regimes of wrought Inconel 718 resulting in four different grain sizes and its effect on EBW. Despite employing the same process parameters, they observe and conclude that weld geometries diverge significantly not only in shape but also in aspect ratio (penetration depth-to-width ratios) by more than a factor of two. Identical conclusions can be drawn after examination of both partial and full penetration weldments. Additionally, they define a relationship between grain size and weld profile. An increase in the grain size of the base metal causes a change of the weld shape: from a stemless wineglass shape, when grains are finer, to a nail head shape with a greater aspect ratio when grain sizes are larger [11].

Jokisch et al. [12] and Rautio et al. [8] published the first fundamental investigations on laser beam welding of L-PBF fabricated Inconel 718 samples. Similar to the investigations of Tavlovich et al. [13] on L-PBF manufactured Ti-6Al-4V, Jokisch's study examines L-PBF manufactured tube sections made of Inconel 718 and Inconel 625 welded by laser and then residual stresses and defects were analyzed. Edge preparation and initial condition (heat treated and not heat treated) of the base material were varied. The investigated samples show an increased porosity, which lead to an rating class C according to DIN EN ISO 13919-1 for most of the samples. The overlap area of the closed circumferential weld is characterized by pore nests, which are, however, considered a characteristic defect for circumferential welds [14]. Stress relief annealing, and mechanical edge preparation of the components are recommended before welding to reduce residual stresses and hence avoid eventual welding defects [12]. Rautio et al. [8] investigates welding characteristics of L-PBF fabricated Inconel 718 samples in as-built, heat-treated, and post-weld heat-treated condition. It is found that in the as-built condition, solidification crack and micropore defects are present in contrast to the heat-treated condition, which do not show such imperfections. Centerline cracks are attributed to the accumulation of high residual stresses from the L-PBF building process and from the laser welding process. He concludes, that they can effectively be avoided by appropriate pre-weld and post-weld heat treatments [8]. Different build-up orientation of the L-PBF samples were not investigated in these two studies.

The microstructure of L-PBF samples in as-built condition is strongly anisotropic owing to the parallel growth of columnar grains to the build direction [15]. The main reason is the strong oriented heat flow during solidification which is highest perpendicular to the surface of pre-deposited layers [16]. Therefore, an investigation of the orientations of the build-up orientation relative to the weld is relevant even after performing some standard heat treatments to the AM samples that can bring partial recrystallization and thus reduce anisotropy [17].

The published investigations have been focused on weldability of both conventional and additively manufactured Inconel 718 and on them very little work has been devoted to deeply analyze the influence of the L-PBF building orientation on the welding process [12].

2. Experimental Procedure

Nickel-based alloy Inconel 718 (2.4668) has been used for all tests and samples. Firstly, commercially available conventional plates of Inconel 718 were procured and additively manufactured specimens of Inconel 718 were fabricated. Conventional samples (80 mm x 25 mm x 7 mm), hereinafter referred to as wrought samples, were obtained from a bigger plate by means of water jet cutting. The procured hot rolled plates were delivered annealed, pickled and heat treated according to the ASTM standard AMS 5596. The two-step aging process consisted of the following steps: Aged at 718 ± 8°C for 8 ± 0.5 hours, then furnace cooled to 621 ± 8°C in 2 hours and then hold at 621 ± 8°C for 8 hours. Finally, air cooled to room temperature. AM samples were fabricated with the L-PBF machine SLM 280HL by SLM Solutions GmbH. For generating the volume of the specimens the following set parameters have been employed: layer thickness of 60 µm, laser power of 350 W (single laser), scan velocity of 800 mm/s, hatch distance of 0.15 mm and a layer-wise rotation of 67°. In order to reduce surface roughness, a border was also printed around the outer hull. This parameter set for the L-PBF process used was provided by the manufacturer of the L-PBF machine. The design strategy and distribution onto the building plate were performed considering guidelines VDI 3405 – Part 3. For a more detailed investigation of building orientation, AM samples were prepared in three different representative building orientation. L-PBF samples have identical dimensions to the wrought ones.

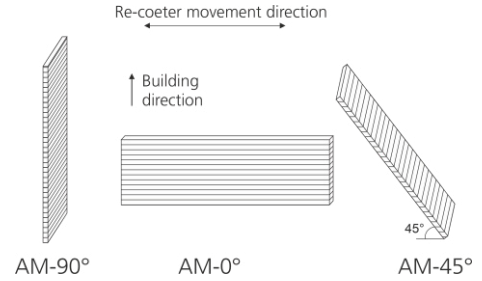

Fig. 1. Building orientation of the fabricated AM samples, AM – 90°, AM – 0° and AM – 45°.

Fig. 1 illustrates the three different building orientations in space. The angle refers to the orientation of the longest edge of printed sample relative to the build platform. The samples were built on a four-millimeter high volume support structure to connect the specimen itself with the building plate. AM samples were stress relieved on the building plate at a temperature of 1065 ± 15°C for 90-5+15 min in accordance with the recommendations suggested by the standard ASTM F3301–18a in order to eliminate any eventual residual stresses generated in the build-up process. No further heat treatment

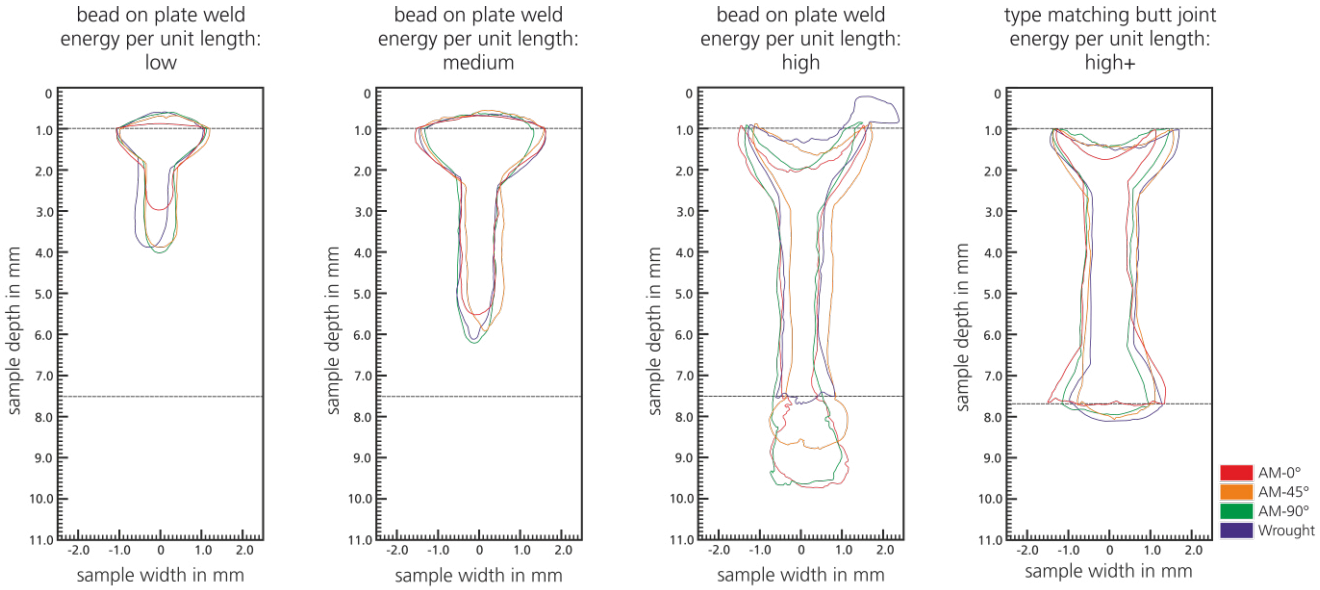

Fig. 2. Graphical superimposition of the weld geometries in cross-section, for the energy per unit *length low*, *medium*, high and, *high+*; ordered by size, the smallest shape is on top.

such as precipitation hardening was performed on the AM samples, for this study.

For the welding tests, bead-on-plate welds were performed on the prepared samples. For comparison, a weld sample was made from a pair of samples as a joint weld for each sample type. Table 1 summarizes the process parameters employed for laser beam welding. Three sets of parameters were investigated for the bead-on-plate welds, which differ in the energy per unit length. For the supplementary joint welds, another parameter set with a higher energy per unit length was applied. The laser employed is a 16 kW Yb:YAG laser by TRUMPF GmbH + Co. KG with a wavelength of 1030 nm and a beam parameter product of 8 mm x mrad. The laser beam is transmitted by an optical fiber with a core diameter of 200 µm.

Table 1. Summary of the welding process parameters applied

Parameter	Unit	Low	Medium	High	High+
Energy per unit length	kJ/cm	0.60	1.20	1.80	2.55
Laser power	W	2000	4000	6000	8500
Welding Speed	mm/min	2000	2000	2000	2000
Focus position	mm	0	0	0	0

Argon is introduced as a protective gas into a nozzle on the underside of the samples and into a chamber on the top of the samples. The samples were cleaned with isopropanol before welding and no further pre-weld operation was executed. Following the welding tests, metallographic cross-sections were obtained from every weld. They were then etched with Kalling's No. 2 etchant. The molten volume of the weld cross-section was digitally measured with a 2.5-fold magnification (numerical aperture 0.8).

3. Results and Discussion

The weld geometry is first measured in detail for each of the specimens to determine the influence of the build-up direction of the AM specimens on the weld geometry. Fig. 2 depicts the area of the molten material as a graphical superimposition. Initially, a distinction can be made between a full penetration for the parameter sets "high" and "high+" and a partial penetration for the parameter sets "low" and "medium". The weld geometry of the partial penetration has a nail-head profile. All welds presented significant porosity within the fusion zone. In addition, it must be mentioned that all samples, but especially the AM samples, show liquation cracks in the necked zone of the nail head like bead cross section, comparable to those described by Shinozaki [9].

Fig. 3. Bright-field image corresponding to a full-penetration bead-on-plate. The base material is an AM-45° sample. The laser beam was directed to the smooth surface (up-skin)

However, there were no centerline solidification cracks as described by Rautio [8]. At an energy per unit length of 1.8 kJ/cm (parameter set "high"), all welds of the AM specimens show a clearly recognizable continuous excessive penetration that results in an excessive melt-through. In regard to the wrought material, a toe overlap at the weld toe is visible. The joints show a comparable weld geometry for all sample conditions, with a clear incompletely filled groove on the top side of the weld. The very low heat input of 0.6 kJ/cm in particular shows a considerable difference between the different build-up orientations of the samples. Especially the

AM-0° samples show a significantly different welding behavior with about 1 mm lower penetration depth compared to all other samples. In addition, the excessive melt-through of the AM samples (parameter set “high”) is deeper than those of the conventional material, being about 1 mm for the AM-45° sample and about 2 mm for both AM-90° and AM-0° samples, which accounts for more than 25% of the plate thickness. Conversely, the overall appearance of the weld welds coincides with the already published investigations [7, 9–11] on the formation of the weld geometry when welding wrought Inconel 718 and is dominated by the selected welding process parameters. Combined with the observation that the deviations of the weld geometry always occur within one parameter set, it can be assumed that the condition of the base material is relevant.

Table 2. Average grain size of the welded samples in base material

	Unit	AM-0°	AM-45°	AM-90°	Wrought
Grain size	µm	200	275	206	30.1

Fig. 4 illustrates the area of molten material relative to the molten area of wrought material for each parameter set. The differences visible in Fig. 2 are quantified in this diagram. Significant deviations of the AM-0° sample at low heat input can equally be recognized, with up to 31% less molten volume for this build-up direction compared to the wrought material. At an energy per unit length sufficient for full penetration welding (parameter set “high”), it can be assessed that the AM samples have molten between 16% to 18% more volume than the wrought material taken as a reference. This observation is consistent with Mei's study on welding wrought Inconel 718 using EBW.

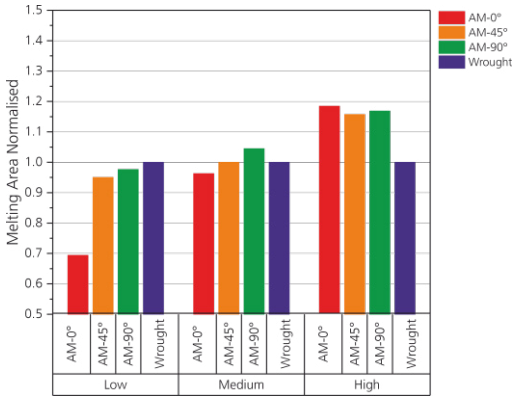

Fig. 4. Relative ratio of the melting area normalized to the respective melting area of the wrought material (=1).

Table 2 summarizes the average grain size of the four different base materials. While the grain sizes of the AM materials in this case range between 200 µm and 275 µm, the average grain size for the wrought samples differs significantly. In addition, it has been already reported that fine grains reduce the risk of cracks along the grain boundaries [18]. A suitable heat treatment of the base material can consequently counteract differing behavior when welding AM and wrought Inconel 718.

The difference in penetration depth for the parameter set “low”, however, cannot be sufficiently explained and will be focus of future studies.

4. Conclusion

The conducted study has documented the profile of the weld geometry as a function of the build-up direction of L-PBF fabricated Inconel 718 specimens and the laser output power when generating the welds.

Under these conditions, significant differences were found among the AM samples and the conventional base material, especially for full penetration welds. It can be concluded that the base material of samples in heat treated condition and the resulting material properties lead to different welding results. Therefore, it is advisable to consider the heat treated condition of the respective base materials before welding pairs of additive manufactured / AM plates or pairs AM – wrought for obtaining final hybrid parts.

Acknowledgements

Funded by the Deutsche Forschungsgemeinschaft (DFG, German Research Foundation) – Project-ID 429808811.

References

[1] Frazier, W. E. Metal additive manufacturing: A review. In: Journal of Materials Engineering and Performance, 6. 2014.

[2] Graf, B., Schuch, M., Kersting, R., Gumenyuk, A., and Rethmeier, M. Additive Process Chain using Selective Laser Melting and Laser Metal Deposition. In: Lasers in Manufacturing Conference. 2015.

[3] Kuryntsev, S. V. The influence of pre-heat treatment on laser welding of T-joints of workpieces made of selective laser melting steel and cold rolled stainless steel. In: Optics & Laser Technology. 2018, S.59–66.

[4] Emmelmann, C. and Beckmann, F. Hybrid lightweight design by laser additive manufacturing and laser welding processes. In *Lasers in Manufacturing Conference 2015*.

[5] Hassanin, A. E., Velotti, C., Scherillo, F., Astarita, A., Squillace, A., and Carrino, L. 2017. Study of the solid state joining of additive manufactured components. In *IEEE RTSI 2017. Research and Technologies for Society and Industry, 3rd International Forum : 2017 conference proceedings : September 11-13 2017 - Modena, Italy*. IEEE, Piscataway, NJ, S.1–4.

[6] B.G. Muralidharan, V. Shankar and T.P.S. Gill. Weldability Of Inconel 718 - A Review. Indira Gandhi Centre For Atomic Research Kalfakkam. 1996.

[7] Odabaşı, A., Ünlü, N., Göller, G., and Eruslu, M. N. A Study on Laser Beam Welding (LBW) Technique: Effect of Heat Input on the Microstructural Evolution of Superalloy Inconel 718. In: Metallurgical and Materials Transactions A, 9. 2010, S.2357–2365.

[8] Rautio, T., Mäkikangas, J., Kumpula, J., Järvenpää, A., and Hamada, A. Laser Welding of Laser Powder Bed Fusion Manufactured Inconel 718: Microstructure and Mechanical Properties. In: Key Engineering Materials. 2021, S.234–241.

[9] Shinozaki, K., Kuroki, H., Luo, X., Ariyoshi, H., and Shirai, M. Effects of welding parameters on laser weldability of Inconel 718. Study of laser weldability of Ni-base, heat-resistant superalloys (1st Report). In: Welding International, 12. 1999, S.945–951.

[10] Xiao, M., Poon, C., Wanjara, P., Jahazi, M., Fawaz, Z., and Krimbalis, P. Optimization of Nd:YAG-Laser Welding Process for Inconel 718 Alloy. In: Materials Science Forum. 2007, S.1305–1308.

[11] Mei, Y., Liu, Y., Liu, C., Li, C., Yu, L., Guo, Q., and Li, H. Effect of base metal and welding speed on fusion zone microstructure and HAZ hot-cracking of electron-beam welded Inconel 718. In: Materials & Design. 2016, S.964–977.

[12] Jokisch, T., Marko, A., Gook, S., Üstündag, Ö., Gumenyuk, A., and Rethmeier, M. Laser Welding of SLM-Manufactured Tubes Made of

IN625 and IN718. In: Materials (Basel, Switzerland), 18. 2019.
[13] Tavlovich B. EBW and LBW of Additive Manufactured Ti6Al4V Products. In: Welding Journal, 6. 2018, S.179–190.
[14] Gook, S., Üstündağ, Ö., Gumenyuk, A., and Rethmeier, M. Avoidance of end crater imperfections at high-power laser beam welding of closed circumferential welds. In: Welding in the World, 2. 2020, S.407–417.
[15] Amato, K. N., Gaytan, S. M., Murr, L. E., Martinez, E., Shindo, P. W., Hernandez, J., Collins, S., and Medina, F. Microstructures and mechanical behavior of Inconel 718 fabricated by selective laser melting. In: Acta Materialia, 5. 2012, S.2229–2239.
[16] Pröbstle, M., Neumeier, S., Hopfenmüller, J., Freund, L. P., Niendorf, T., Schwarze, D., and Göken, M. Superior creep strength of a nickel-based superalloy produced by selective laser melting. In: Materials Science and Engineering: A. 2016, S.299–307.
[17] Chlebus, E., Gruber, K., Kuźnicka, B., Kurzac, J., and Kurzynowski, T. Effect of heat treatment on the microstructure and mechanical properties of Inconel 718 processed by selective laser melting. In: Materials Science and Engineering: A. 2015, S.647–655.
[18] Tharappel, J. T. and Babu, J. Welding processes for Inconel 718- A brief review. In: IOP Conference Series: Materials Science and Engineering. 2018, S.12082.